Confined-Direct Electric Curing of NaOH-activated fly ash based brick mixtures under free drainage conditions: Part 1. Factorial experimental design

Mateusz Ziolkowski[a]*, Maxim Kovtun[a]

[a]Department of Civil Engineering, University of Pretoria, Pretoria, 0002 South Africa

mateusz.zski@gmail.com (M Ziolkowski)

max.kovtun@up.ac.za (M Kovtun)

*Corresponding author at: Department of Civil Engineering, University of Pretoria, Pretoria, 0002 South Africa. Tel.: +27 78 765 4554. E-mail address: mateusz.zski@gmail.com (M Ziolkowski)

Abstract

The utilisation of fly ash is a global concern. Under conditions of mass production and rapid turnover in automated plants, a reduction in the curing duration of alkali-activated fly ash based mixtures is sought-after. An alternative accelerated curing technique, confined-DEC (Direct Electric Curing), with the binding mechanism of NaOH activation of fly ash was investigated for the rapid manufacture of fly ash based bricks. This concept is a potentially viable alternative solution for high-volume fly ash utilisation. The investigation revealed that the confined-DEC technique shows great promise in the rapid accelerated curing of NaOH-activated fly ash based brick mixtures. The best induced design conditions, a mixture consisting of 4.1% NaOH, 9% water and 86.9% fly ash by weight, simultaneously subjected to a confining pressure of 10 MPa and a voltage gradient of 0.8 V/mm, obtained a compressive strength of 11.5 MPa in 7 minutes and the mixture continued to increase in compressive strength after the application of confined-DEC, acquiring a compressive strength

of 20.1 MPa at 28 days. The investigation also revealed the limitations of confined-DEC under free drainage conditions.
Keywords: Alkali-Activated; Fly Ash; Confined-Direct Electric Curing; Acceleration; Brick; Compressive strength; Factorial design; Free drainage conditions.

1. Introduction

South Africa alone produces 40 million tons of coal ash per annum, of which approximately utilises only 7% of fly ash generated and the rest, including bottom ash, is stacked on dumps or ash dams, creating landfills [1]. Economic factors increasingly dictate that the industry should look towards recycling waste materials as opposed to landfilling and discarding [2]. Increase in production of fly ash across the globe compels one to increase the utilization of fly ash in the construction industry [3]. One significant way to make use of waste in large quantities is by utilising it in brick manufacture [4]. The utilization of fly ash to manufacture bricks can not only solve the storage and enviromental issues, but also reduce the exploitation of natural resources for brick production, for example, clay. Traditional brick manufacturing methods, firing process, consumes significant amount of energy and releases large quantity of greenhouse gases [5]. Today low-temperature accelerated curing techniques below 150 °C are possible and favourable since they are not as energy intensive as firing, and are capable of producing adequate fly ash based bricks [6, 7].

Liu et al., (2005) [8] successfully manufactured bricks from high-calcium fly ash without the addition of a cementing agent. However, most South African fly ashes are low-calcium content [9], which has low self-cementing properties. Therefore, the addition of a cementing agent is needed, but regular cementing methods for producing bricks from waste materials have the disadvantages of high energy consumption and a large carbon footprint [5]. Using geopolymerisation to produce bricks from waste materials currently seems to be the most

prevalent way to address energy and environmental concerns [5]. However, geopolymer binding technology used in fly ash mixtures is frequently associated with conventional thermal curing. The main drawback of conventional thermal curing is that it inevitably increases the energy consumption, offsetting the benefits that can be obtained from alkali-activated fly ash [10]. It is possible to synthesise an alkali-activated fly ash based binder at an ambient temperature, but it is impractical, due to delayed setting, intensive efflorescence formation, very slow mechanical strength development and relatively low strength at 28 days of age [11].

As with the traditional firing process, low temperature curing is also governed by long curing durations. With conventional heating techniques, heat is distributed in the specimen from the exterior to the interior leading to a uniform and long heating period to attain the required temperature [12]. Ahmari and Zhang (2012) [13] successfully manufactured adequate bricks from waste (taillings) through geopolymerisation, but their brick mixtures were oven cured for 7 days. The long duration of curing also does not aid the successful utilisation of fly ash. Under conditions of mass production and rapid turnover in automated plants, reduction in curing duration is sought-after. The temperature rise in conventional masonry units during curing is limited to a rate of 20 °C/hour [14]. The coefficients of thermal expansion for aggregates and cement are of the same order of magnitude, but for water it is roughly 15 times, and for air 200 times, higher [15]. The different expansion characteristic of the constituents leads to differential expansion during curing, resulting in generated stresses within the mixture. Beyond the recommended curing rate, the early strength of concrete masonry units is not enough to counteract the generated stresses; cracks are formed from within the mixture, resulting in reduced later strength [15].

Compared to conventional thermal curing, such as oven curing, it is generally agreed that microwave curing is a low-energy heating source [10]. Chindaprasirt et al. (2013) [12] showed that early-stage microwave curing followed by conventional oven curing reduced the

curing duration and energy consumption and, hence, the associated cost. However, mixtures prepared with microwave curing are also prone to thermally induced cracks at high heating rates. Somaratna et al. (2010) [16] observed severe cracking and deterioration within a few minutes of alkali-activated fly ash mixtures subjected to too high power levels of microwave curing.

An accelerated curing technique investigated by Davidovits and Legrand (1977) [17] shows that rapid hardening of a mixture in a matter of minutes is possible. A semi-dry mixture within a mould was compressed between two heated plates at 150 °C, and within minutes the strength of the material was approximately the same as a similar mixture that was cured in an oven for 1.5 hours at the same temperature, 150 °C. This rapid accelerated curing was possible because the two heat plates suppressed the formation of cracks by preventing differential expansion within the mixture.

With the confinement of the mixture, curing duration is not governed by heating rates. However, one drawback of this curing technique by Davidovits and Legrand (1977) [17] is that it becomes ineffective for thicker mixtures. The semi-dry mixture that hardened in 3 minutes was only 3 mm thick, the redistribution of the heat from the plates into the mixture was rapid. However, the redistribution of heat will take longer with an increase in mixture thickness, especially with brick mixtures. Therefore, this curing technique is not as effective as conventional curing techniques when thicker elements are being cured.

This rapid accelerating curing of materials for thicker mixtures can simply be overcome by replacing the heated plates with another source of heat, with Direct Electric Curing (DEC). This method utilises the properties of the mixture to generate heat, and not its surroundings.

In DEC, an alternating electric current is directly induced through a mixture of relatively high resistivity between two imbedded electrodes, and during this process heat volumetrically rises throughout the mixture, and also in a shorter time [15]. This heating mechanism is also known as Joule heating and ohmic heating; under the influence of an electric field, the

resistance that the moving ions encounter results in the generation of heat. Alternating current is used to avoid the electrolysis of the mixture [18] and, generally, mains frequency supplies of 50 Hz are used for DEC [19]. Otherwise, under direct current (0 Hz), the formation and liberation of hydrogen gas at the electrodes results in the polarisation of the electrodes, which obstruct the flow of charges to the electrode surface [19; 20; 21]. This problem is eliminated by the use of alternating current [19; 20; 21].

The limitations encountered during the heated plate curing technique do not occur with DEC; current flow input is adjusted to the thickness of the element. DEC is also one of the most energy-efficient methods for accelerated curing [21, 22]. The combination of confinement and DEC, confined-DEC, introduces a potentially novel approach in rapid accelerating curing of masonry units. Confined-DEC, keeps the confinement aspect of Davidovits and Legrand's (1977) [17] method, but replaces the heated plates with electrodes.

This curing approach, confined-DEC, can also support mass production of fly ash bricks on an industrial scale. Fly ash does not have the physical plastic properties [23] to be extruded from a rectangular die like clay [24], which are commonly manufactured on a large scale. Belden et al. (2012) [25] explain that in order to commercialise bricks with more than 40% coal ash, it becomes necessary to press mould the brick mixture. Hence, on an industrial scale, confinement of the mixture and DEC can be introduced during the press moulding of fly ash based mixtures.

The semi-dry mixture mentioned earlier, which hardened in a manner of minutes, is what is known today as an 'alkali-activated material': kaolinite mixed with a solution of NaOH. Based on the findings by Davidovits and Legrand (1977) [17], with the appropriate induced curing conditions, the rapid manufacture of alkali-activated materials is possible. Of the two most commonly used alkali activators, NaOH and sodium silicate [26], NaOH-activated fly ash based mixtures have a smaller carbon footprint than sodium silicate-activated fly ash based mixtures [27]. Bakharev (2005) [28] observed that fly ashes activated with NaOH had more

stable strength properties at later ages than fly ashes activated with sodium silicate. Previous work revealed that the NaOH present in the alkali activator provided an adequate conductive medium for generating heat in accelerated curing of NaOH-activated fly ash concretes [29]. The combination of confinement and DEC – confined-DEC – with the binding mechanism of NaOH activation of fly ash indicates that this novel approach in the rapid manufacture of bricks could be a viable alternative solution for high-volume fly ash utilisation.

The paper consists of two parts: Part 1: Factorial experimental design, and Part 2: Confined-DEC versus oven curing. The findings of Part 1 are presented in this paper. The objective of Part 1 is to investigate the capability of confined-DEC to rapidly manufacture NaOH-activated fly ash based brick mixtures of adequate compressive strength and also to provide insight into the influence of variables on rapid compressive strength development and the limitations of confined-DEC.

2. Experimental procedure and material properties

2.1. Experimental set-up

For safety reasons, the design of the confined-DEC set-up is based on the design of Davidovits and Legrand (1977) [17] with regards to relieving the internal water pressure build-up during curing; the compressed material is allowed a capillarity migration of water (free drainage conditions). This prevents dangerous steam outbursts when the confining pressure is removed after curing. Otherwise, in a closed system (un-drained conditions), time must be allowed for the mixture to cool down to a safe temperature before the mould can be opened, though this increases the total curing duration. The confined-DEC set-up was designed to produce three 50 mm cubes, in order to obtain statically significant results in compressive strength development.

Fig. 1 represents the sectional view of the centre mould of the confined-DEC device. The following description of the design corresponds to the legend provided in Fig. 1. The electric cable (1) supplies the power to the electrodes, which are connected to a voltage regulator. The purpose of the primary body (3), which consists of 20 mm-thick mild steel, is to handle the high pressure generated during the compaction of the mixture and the pressure generated during curing. The secondary body (4), which is non-conductive, is present to break the conductivity between the electrodes and to force the current to flow through the mixture between the electrodes. Otherwise the electric current would flow through the steel body.

The bottom electrode (11) is attached to a non-moving assembly. The bolt (8) and the conductive element (14) maintain the electric connection between the electrode (11) and the electric cable (1). The conductive element (14) also acts as a heat sink during curing. The thermocouple (15) embedded in the conductive element (14) measures the change in temperature; this type of set-up allows for a non-influential measuring technique on the physical properties of the mixture (13) being cured. Although this will not provide the true temperature of the mixture during curing and will contribute to some heat loss, it will provide an indication of the relative change of temperature curves between experiments. The non-conductive element (16) completing the bottom assembly also prevents heat dissipation. The non-conductive element (18) keeps the bottom assembly in position, provides a drainage path outwards and isolates the surroundings from the live current.

The top assembly is a free moving assembly; it moves under the load induced by the hydraulic piston (2) during compaction of the mixture (13). The bolt (8) and the conductive element (10) also keep the electric connection between the electrode (11) and the electric cable (1). The point of the free moving block (7) is to prevent possible rotation or wedging of the thinner elements (the electrode (11) and the conductive element (10)) during compaction. The non-conductive element (9) prevents massive heat absorption by the free mild steel moving block (7), which also acts as a safety feature by prolonging the drainage path for

steam bursts. The non-conductive element (5) isolates the hydraulic piston (2) from the electric current.

The drainage paths (12) run vertically upwards along the sides of the top assembly and also vertically downwards along the sides of the bottom assembly. The drainage paths of the bottom assembly lead into the drainage path imbedded in the non-conductive element (18), which leads out of the mould.

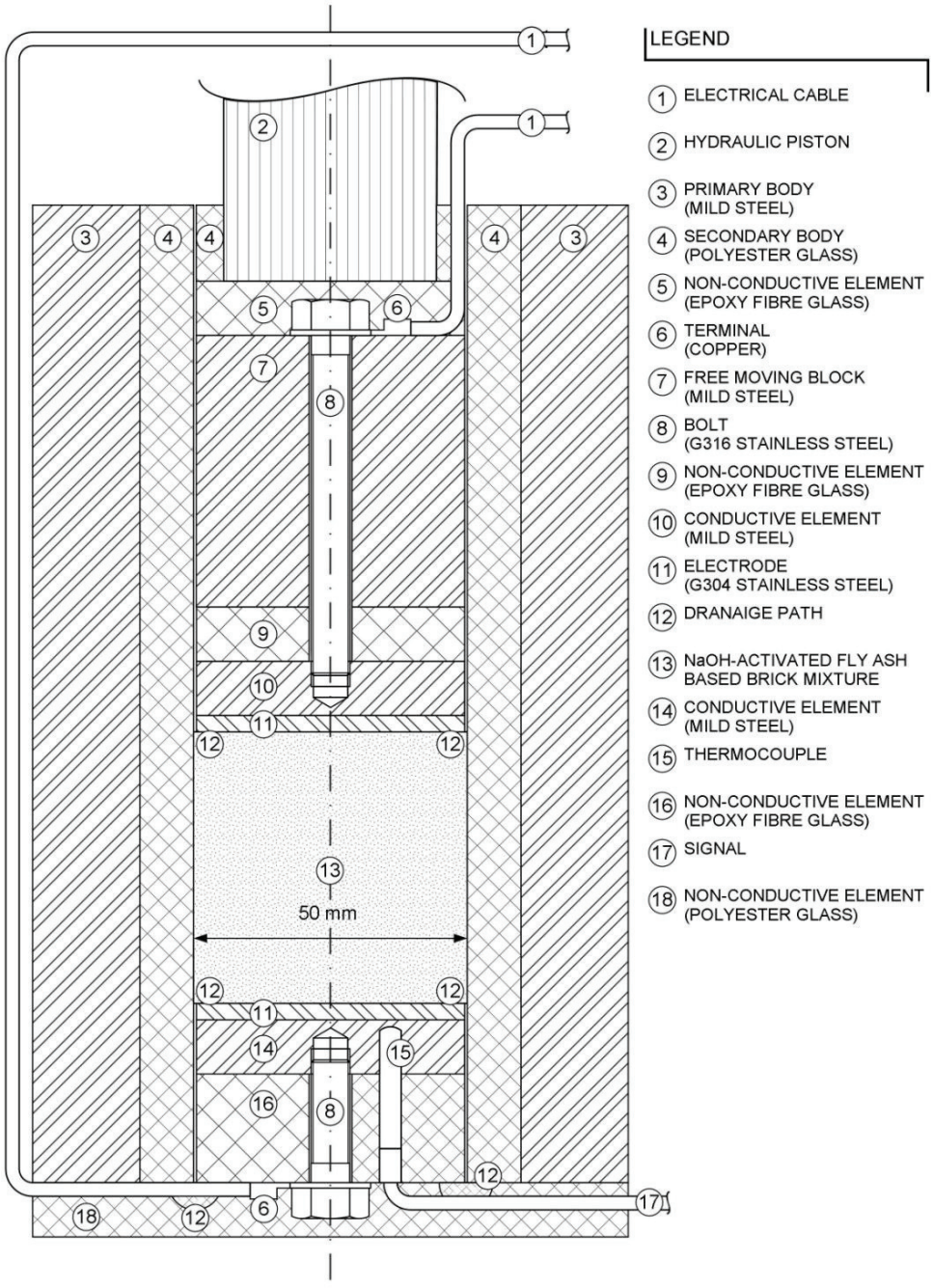

(One and a half page width, 140 mm, fitting image)

Fig. 1. Cross sectional view of the confined-DEC device.

A simplified schematic of the electric set-up is depicted in Fig. 2. The moulds were connected in series and not in parallel to prevent unequal current flow in case the conductivity broke within any of the mixtures during curing. Once the conductivity breaks within one mixture, the electric current is kept from flowing into the other cubes, which ensures that all the mixtures receive the same amount of electric current.

The power supply, 240 V 50 Hz, was connected to an ACDC Dynamics voltage regulator (step-down transformer) with a regulated output voltage of 0-250 V. Current (A) and voltage (V) were measured with a Rhomberg Digital Ammeter and a Rhomberg Digital Voltmeter, respectively. For temperature measurement, a Rhomberg TC600 Temperature Controller was used in conjunction with an attached thermocouple.

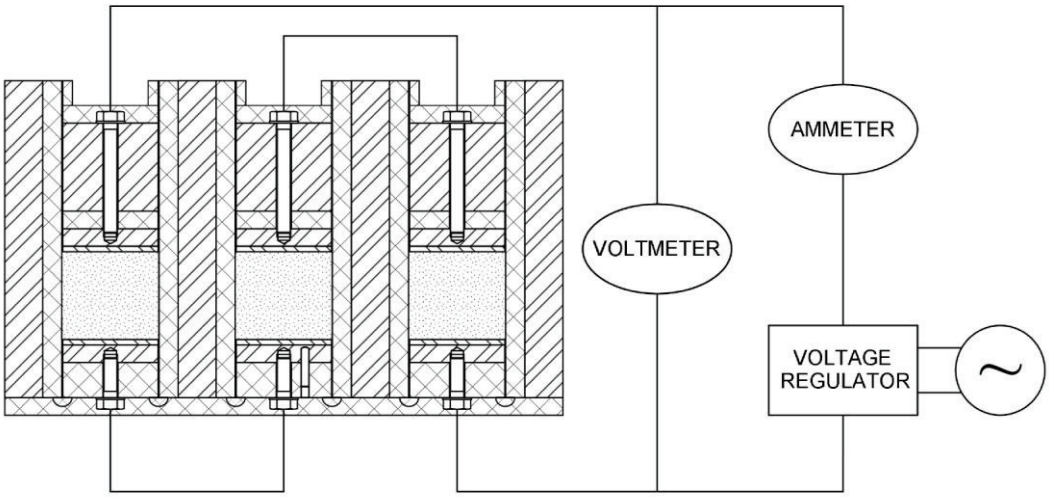

(One and a half page width, 140 mm, fitting image)

Fig. 2. Simplified schematic of the electric set-up; the symbol "~" indicates alternating current source.

To reduce the variability in the pressure applied to moulds, Whissell (1989) [30] describes a method which uses multiple hydraulic cylinders; each hydraulic cylinder compacts its

respective mixture. The hydraulic cylinders are connected to the same hydraulic fluid line, which is connected to one pressure fluid source, a hydraulic jack. During the compaction of the multiple mixtures, the fluid pressure is equal everywhere in the hydraulic fluid line and, therefore, the pressure induced by the cylinders on the mixtures is also equal.

The compaction set-up is placed in-between the top segment and the bottom base of the SANS Hydraulic Universal Testing Machine. The placement of the compaction set-up in the SANS Hydraulic Universal Testing Machine not only forces the load to go through the mixture during compaction but also measures the amount of axial compression force induced in-between the top segment and the base. The desired pressure is back-calculated in terms of force, and then the mixture is compacted until the desired force is reached.

2.2. Materials

A classified fly ash was used throughout the investigation. The average density and Blaine fineness of the classified fly ash was 2240 kg/m^3 and 316 m^2/kg respectively. The classified fly ash complies with the chemical and physical requirements of BS EN450, ASTM C618 and all relevant international quality standards for fly ash. The chemical composition of fly ash is shown in Table 1. The particle size distribution of the fly ash is depicted in Fig. 3. Commercially available NaOH flakes (98.0 % purity) and tap water were used to prepare NaOH solutions.

Table 1

Chemical composition of fly ash (weight %)

SiO_2	Al_2O_3	CaO	Fe_2O_3	TiO_2	MgO	K_2O	P_2O_5	Other	LOI
54.9	31.5	4.5	3.5	1.6	1.0	0.8	0.4	0.3	1.0

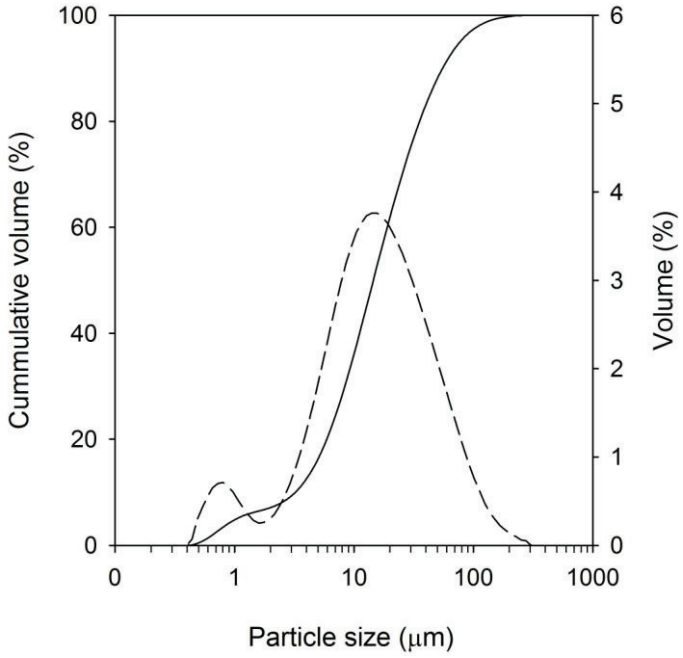

(Single column, 90 mm, fitting image)

Fig. 3. Particle size distribution of the fly ash

2.3. Experimental design

In the exploration of an unknown system, a strategic experimental design is essential in order to recognise the influence of each variable and variable interaction on the compressive strength development of a NaOH-activated fly ash brick mixture subjected to confined-DEC. The guideline for designing an experiment provided by Montgomery (2012) [31] was used to build an empirical model of the investigated system.

2.3.1. Response variable and variable level selection

In this experimental design, the selected response is the average of three compressive strength tests right after the NaOH-activated fly ash mixture has been subjected to confined-DEC. Mechanical properties in terms of compressive strength development are a good indicator of the reaction degree of the final product, alkali aluminosilicate gel [32]. The samples were

crushed at a 15 MPa/min rate, as prescribed by the South African concrete masonry unit standard (SANS 1215:2008) [33]. The following four variables were considered to have a significant impact on the variability of the compressive strength development: total water content, voltage gradient, confining pressure and sodium oxide (Na_2O) content.

Total water content is defined as the weight ratio of water (kg) to the solid constituents (kg) of the mixture (fly ash and NaOH solids), given as a percentage. Total water content has two roles during curing: it acts as a medium for alkali activation of fly ash to proceed [34] and as a medium for the current to flow through, for Joule heating purposes. A too low water content will result in poor formation of the alkali aluminosilicate gel and provide poor conductivity for electric current to flow through. In contrast, a high water content will lead to a squeezing out of Na^+ and OH^- ions with water; Ahmari and Zhang (2012) [13] observed this occurrence. A high water content also increases the overall specific heat of the mixture; more electric energy is absorbed in a wetter mixture than in a drier mixture with the same temperature rise [15]. As found during experimental work, compressive strength development decreased when the total water content was increased from 11% to 13% and from 13% to 17%, indicating the squeezing out of Na^+ and OH^- ions with water during compaction [13]. Therefore, the maximum total water content was limited to 10%.

The electric current will induce the heating mechanism (Joule heating). An increase in current flow will correspond to an increase in heating rate. During the experimental work conducted in the study, a voltage gradient of 1.2 V/mm and higher resulted in the mixture having explosive nature through steam bursts within 2 minutes of subjecting the mixture to confined-DEC. This also produced poor samples. Due to safety concerns and production of poor-quality NaOH-activated fly ash samples, the maximum voltage gradient was limited to 1.0 V/mm.

As found during experimental work, the compaction of the mixture to 15 MPa and higher played a small role on the variability of compressive strength development for mixtures

having low total water content. The notable influence of confining pressure was found below 15 MPa.

The equivalent NaOH concentration is expressed in terms of Na_2O. Na_2O content is defined as the weight ratio of Na_2O (kg) to the fly ash (kg) from the binder, given as a percentage. Na_2O content serves a dual role during curing: carrying the electric current for Joule heating purposes [29] and taking part in the alkali activation of fly ash [35]. There is a critical range for the conductivity of the alkaline solution in order for Joule heating to be effective. To successfully generate the amount of heat that is required for the Joule effect to take place, conductivity that is too low will need large voltages, and conductivity that is too high will need large amperages [36].

2.3.2. Choice of experimental design and mixture design

To accommodate the possible presence of curvature in the studied system, a second-order model was considered. The level and range of the four variables considered are shown in Table 2. The axial-value for a 2^4 variable central composite design is 2. Using the information from Table 2, a generated 2^4 central composite design is given in Table 3. The first sixteen trial runs in standard order are factorial points. The next eight trial points are axial points and the last six trial points are centre runs. The replication of the centre runs provides an estimate of experimental error. The central composite design was executed in random order to ensure that conditions in one run neither depend on the conditions of the previous run nor influence the conditions in the subsequent run.

The mixture design for each factorial design point, given in Table 3, was based on the level of variables established in the 2^4 central composite design (Table 2). The mixture designs consisted of two parts: binder and aggregate. The binder part consisted of fly ash, water and NaOH, and the aggregate part only of fly ash. As the high utilisation of fly ash is important,

the aggregate part consisted of the same type of fly ash that was used in the binder. An increase in the proportion of binder to aggregate would result in an increase in compressive strength development to a certain extent, since the NaOH content is systematically also increased. However, for economical reasons with regards to keeping the NaOH content low, a sufficient binder content of 18% [37] by volume was kept constant for all the design points investigated. Ravikumar et al., (2010) [37] found that a binder content of 18% by volume was the optimum content in the manufacture of alkali-activated fly ash based concrete mixtures.

Table 2

Coded and actual values of 2^4 central composite design

			Levels of code				
			Axial low	Low	Centre	High	Axial high
Independent variable	Code	Units	-2	-1	0	+1	+2
Total water content	A	%	6	7	8	9	10
Voltage gradient	B	V/mm	0.2	0.4	0.6	0.8	1.0
Confining pressure	C	MPa	2.5	5	7.5	10	12.5
Na_2O content	D	%	1	6	11	16	21

Table 3

The generated 2^4 central composite design with corresponding mixture design

2^4 central composite design						Mixture design			
						Binder			Aggregate
Standard/	Total water content	Voltage gradient	Confining pressure	Na_2O content		Fly ash	NaOH	Water	Fly ash
Run order	(%)	(V/mm)	(MPa)	(%)	Identification label	(kg/m^3)	(kg/m^3)	(kg/m^3)	(kg/m^3)
1/18	7	0.4	5	6	7|0.4|05|06 (E01)	403	31	146	1500
2/13	9	0.4	5	6	9|0.4|05|06 (E02)	403	31	183	1416
3/11	7	0.8	5	6	7|0.8|05|06 (E03)	403	31	146	1500
4/23	9	0.8	5	6	9|0.8|05|06 (E04)	403	31	183	1416
5/15	7	0.4	10	6	7|0.4|10|06 (E05)	403	31	146	1500
6/26	9	0.4	10	6	9|0.4|10|06 (E06)	403	31	183	1416
7/21	7	0.8	10	6	7|0.8|10|06 (E07)	403	31	146	1500
8/14	9	0.8	10	6	9|0.8|10|06 (E08)	403	31	183	1416
9/30	7	0.4	5	16	7|0.4|05|16 (E09)	403	83	146	1455
10/19	9	0.4	5	16	9|0.4|05|16 (E10)	403	83	184	1371
11/10	7	0.8	5	16	7|0.8|05|16 (E11)	403	83	146	1455
12/01	9	0.8	5	16	9|0.8|05|16 (E12)	403	83	184	1371

13/02	7	0.4	10	16	7|0.4|10|16 (E13)	403	83	146	1455
14/06	9	0.4	10	16	9|0.4|10|16 (E14)	403	83	184	1371
15/08	7	0.8	10	16	7|0.8|10|16 (E15)	403	83	146	1455
16/25	9	0.8	10	16	9|0.8|10|16 (E16)	403	83	184	1371
17/05	6	0.6	7.5	11	6|0.6|7.5|11 (E17)	403	57	126	1518
18/16	10	0.6	7.5	11	10|0.6|7.5|11 (E18)	403	57	201	1351
19/20	8	0.2	7.5	11	8|0.2|7.5|11 (E19)	403	57	165	1433
20/03	8	1.0	7.5	11	8|1.0|7.5|11 (E20)	403	57	165	1433
21/17	8	0.6	7.5	11	8|0.6|2.5|11 (E21)	403	57	165	1433
22/27	8	0.6	12.5	11	8|0.6|12.5|11 (E22)	403	57	165	1433
23/07	8	0.6	7.5	1	8|0.6|7.5|01 (E23)	403	5	163	1470
24/04	8	0.6	7.5	21	8|0.6|7.5|21 (E24)	403	109	165	1386
25/29	8	0.6	7.5	11	8|0.6|7.5|11 (E25)	403	57	165	1433
26/28	8	0.6	7.5	11	8|0.6|7.5|11 (E26)	403	57	165	1433
27/12	8	0.6	7.5	11	8|0.6|7.5|11 (E27)	403	57	165	1433
28/22	8	0.6	7.5	11	8|0.6|7.5|11 (E28)	403	57	165	1433
29/09	8	0.6	7.5	11	8|0.6|7.5|11 (E29)	403	57	165	1433
30/24	8	0.6	7.5	11	8|0.6|7.5|11 (E30)	403	57	165	1433

2.2.3. Statistical analysis procedure

The general approach to the statistical analysis of the 2^k design provided by Montgomery (2012) [31] was applied. The approach goes as follows: form initial model, perform statistical testing (ANOVA), refine model, analyse residuals and interpret results. A computer software, Design-Expert® 10.0, was used to assist with the design, statistical analysis and interpretation of the 2^4 central composite design.

2.4. Mixture preparation

In preparation of the mixture, firstly, the NaOH solids were mixed with tap water and left to cool down to room temperature. The NaOH solution was then mixed with the fly ash binder for 10 minutes. Rattanasak and Chindaprasirt (2009) [38] found that mixing fly ash with a NaOH solution of 10 M for 10 minutes allowed the maximum leaching yield of Si^{4+} and Al^{3+} species; these are important species in the formation of an alkali aluminosilicate gel.

Although the molar concentration of the NaOH solution differs between factorial design points, the mixing time was kept to 10 minutes. Afterwards, the binder was mixed for a further 5 minutes with the fly ash aggregate at a slower speed.

A shortage of water can lead to the prevention of fully dissolving the glass component of fly ash, the first stage of the cementitious gel formation [39]. The water content range considered in this investigation produced considerably dry mixtures; when all the fly ash (binder and aggregate) was mixed with the NaOH activator at once, the fly ash particles were not fully immersed in the NaOH activator. The mixture resembled that of a powder like consistency. However, the mixture preparation procedure ensured that at least the fly ash from the binder part was fully immersed in the NaOH activator, and the 10-minute contact time ensured the maximum yield of desirable species for the formation of the alkali aluminosilicate gel [38]. During this step, the mixture resembled that of a slurry and, afterwards, with the addition of the aggregate, the mixture resembled that of a powder like consistency.

2.5. Sample preparation

In preparation of the samples, firstly, the mixture was cast into the confined-DEC set-up (three casts), then compacted to a specific pressure and subjected to a specific voltage gradient, as stated by the factorial design point being investigated. Once the curing duration was over, the electric current was switched off and the pressure relieved. The cured samples were demoulded and tested for compressive strength.

Curing duration was based on utilising the full potential of the mixture's Joule heating capability in the shortest possible duration. The first indication that the mixture's Joule heating capability became ineffective during curing was when the measured temperature started dropping after a maximum temperature was reached. The dropping temperature signified that the mixture’s Joule heating capability was no longer effective in generating

heat. This was also supported by the measured current flow. Initially, the electric current flow increased during curing; this signified that the temperature of the conductive medium was also increasing. However, once a maximum current was reached, a drastic drop followed and the current flow settled at a lower current flow than the initial one. The change in current flow indicated that physical changes were occurring during curing, either through water movement, chemical reactions or both. When the current flow settled, it meant that the mixture's ability to generate heat had become ineffective, which also coincided with the measured temperature dropping. Therefore, curing was stopped after the drop in temperature was observed. Some factorial design points had poor Joule heating capabilities, the temperature stopped rising (0 °C/minute) after a certain period. This indicated that the mixture's heating capability was not effective. After a period of 20 minutes with no change in temperature, the curing was stopped.

3. Results and discussion

3.1. 2^4 Central composite design

3.1.1. Generated response

The average measured response, compressive strength development, of each design point from the 2^4 central composite design is presented Fig. 4. It is evident that the different combinations of variables at different levels, high and low, generated a unique response for each design point. A minimum and maximum compressive strength of 0.1 MPa and 11.5 MPa respectively were generated.

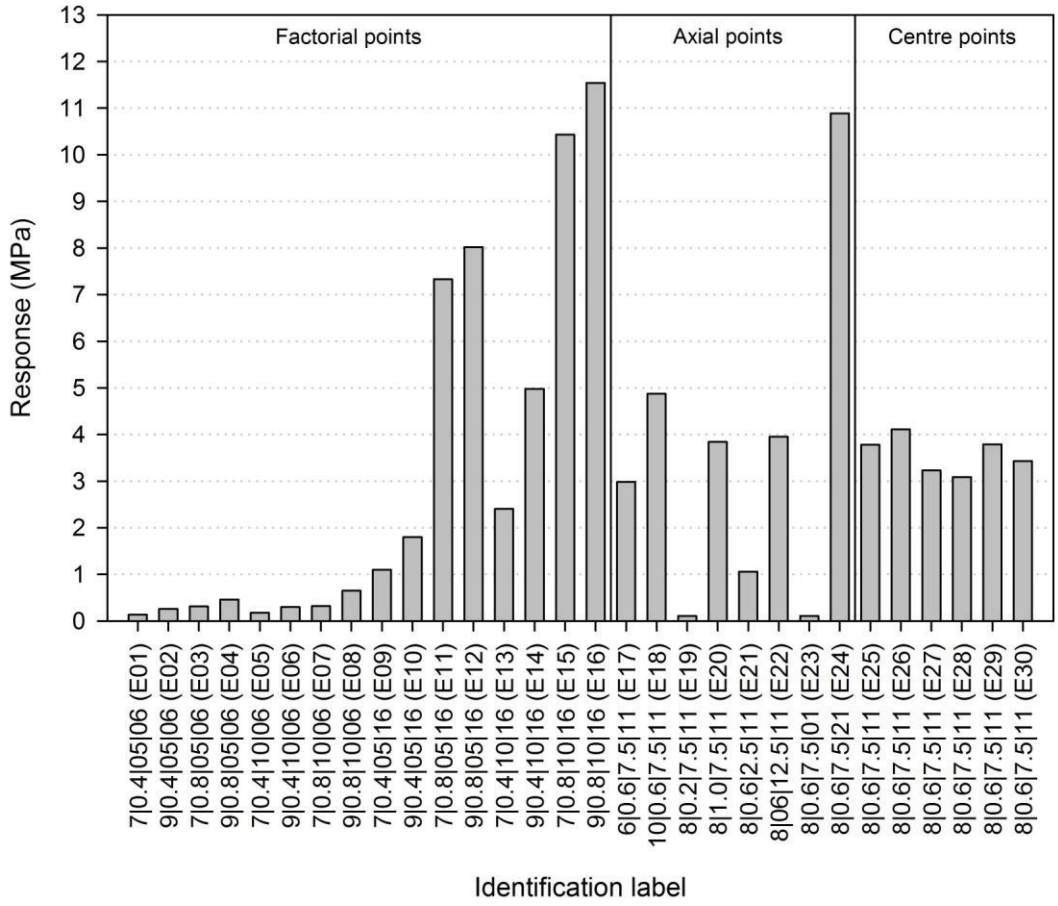

(One and a half page width, 140 mm, fitting image)

Fig. 4. The average measured response of each design point from the 2^4 central composite design.

3.1.2. Model fitting and validation

The response was initially analysed without a transformation, but the diagnosis of the residuals revealed violations of the least squares regression assumptions. In the normal probability plot of the studentised residuals, an s-shape was present; the non normality assumption was not satisfied. In the plot of externally studentised residuals, two residuals plotted outside the 95% confidence limits; the presence of outliers suggested that the experimental runs did not agree well with the considered model. The transformation of the response variable frequently provides a remedial to the violated assumption mentioned and other problems (outliers). The generated response ranges from 0.1 to 11.5 MPa; the ratio

between the maximum and minimum response is greater than 10. A ratio greater than 10 usually indicates that a transformation is required [40]. Based on the Box-Cox plot from Design-Expert® 10.0, the response was re-analysed with a square-root transformation. The initial model suggested by Design-Expert® 10.0 was a full quadratic model. The model consisted of first- and second-order terms as well as two-factor interactions terms (A, B, C, D, AB, AC, AD, BC, BD, CD, A^2, B^2, C^2 and D^2). The analysis of variance (ANOVA) was applied to formally test the significance of the considered model. ANOVA confirmed the adequacy of the model; the *F*-value of 65.83 implied that the model is significant. There was only a 0.01% chance that an *F*-value this large could occur due to noise. However, insignificant model terms were still present in the full model.

In the next step, the least significant model terms were removed one at a time until the least significant term remaining had a p-value less than 0.05. Table 4 shows the ANOVA of the reduced model. Model terms A, B, C, D, BD, CD, B^2 and C^2 are still significant after model term refinement. The lack of fit *F*-value of 2.95 implies that the lack of fit is not significant relative to the pure error. There is an 11.84% chance that a lack of fit *F*-value this large could occur due to noise. The non-significant lack of fit is good.

Table 5 provides the summary statistics of ANOVA. The ordinary R^2 indicates that the model explains about 97.88% of total variability. The predicted R^2 indicates that the model will probably explain approximately 94.46% of the variability in the new data. The predicted R^2 of 94.46% is in agreement with the adjusted R^2 of 97.07%, as they are within 0.2 of each other [40]. It is very unlikely that non-significant terms have been included in the model. The adequate precision of 38.02 is satisfactory, as an adequate precision greater than 4 is desirable [40]. The overall capability of the model, based on these criteria seems very satisfactory.

Table 4
ANOVA for reduced quadratic model [Partial sum of squares - Type III]

Source	Sum of Squares	df	Mean Square	*F*-value	*p*-value Prob> F	
Model	25.28	8	3.16	121.19	< 0.0001	Significant
A-Total water content	0.34	1	0.34	12.94	0.0017	
B-Voltage gradient	4.17	1	4.17	159.72	< 0.0001	
C-Confining pressure	0.89	1	0.89	34.12	< 0.0001	
D-Na_2O content	16.36	1	16.36	627.28	< 0.0001	
BD	1.72	1	1.72	65.82	< 0.0001	
CD	0.32	1	0.32	12.20	0.0022	
B^2	1.24	1	1.24	47.51	< 0.0001	
C^2	0.40	1	0.40	15.18	0.0008	
Residual	0.55	21	0.03			
Lack of Fit	0.50	16	0.03	2.95	0.1184	Not significant
Pure Error	0.05	5	0.01			
Cor Total	25.83	29				

Table 5

Summary statistics

Standard Deviation	Mean	C.V. %	PRESS	R^2	Adjusted R^2	Predicted R^2	Adequate Precision
0.16	1.57	10.31	1.43	0.9788	0.9707	0.9446	38.02

The diagnosis of the residuals revealed no violation of least squares regression assumptions. The residuals follow a straight line in the normal probability plot of the studentised residuals. No megaphone shape is present in the plot of studentised residuals versus the predicted response. No apparent trend is present in the plot of the residuals versus the experimental run order. In the plot of externally studentised residuals versus run number; all data values are plotted within the 95% confidence limits. None of the studentised residuals are large enough to indicate any problems with outliers and the experimental runs agreed well with the current model. With all the model statistics and the diagnosis of residuals satisfied, the final model can be used to navigate the design space.

3.1.3. Model interpretation

The final empirical model for predicting the compressive strength development of the generated response is given in terms of coded and actual variables by Equation (1) and Equation (2) respectively. Coded variables in Equation (1) make the interpretation of the empirical model easier because the magnitudes of the coefficients are given on a common scale.

$$Y = (+1.83 + 0.12 \cdot A + 0.42 \cdot B + 0.19 \cdot C + 0.83 \cdot D + 0.33 \cdot B \cdot D + 0.14 \cdot C \cdot D - 0.21 \cdot B^2 - 0.12 \cdot C^2)^2 \quad (1)$$

Where Y – Compressive strength (MPa);

A – total water content (%), -1 ≤ A ≤ +1;

B – voltage gradient (V/mm), -1 ≤ B ≤ +1;

C – confining pressure (MPa), -1 ≤ C ≤ +1;

D – Na_2O content (%), -1 ≤ D ≤ +1.

$$= (-2.61 + 0.12 \cdot A + 4.74 \cdot B + 0.24 \cdot C - 0.12 \cdot D + 0.33 \cdot B \cdot D + 0.01 \cdot C \cdot D - 5.22 \cdot B^2 - 0.02 \cdot C^2)^2 \quad (2)$$

Where Y – Compressive strength (MPa);

A – total water content (%), 7 ≤ A ≤ 9;

B – voltage gradient (V/mm), 0.4 ≤ B ≤ 0.8;

C – confining pressure (MPa), 5 ≤ C ≤ 10;

D – Na_2O content (%), 6 ≤ D ≤ 16.

The empirical model clearly indicates that all variables employed in the central composite design contribute to compressive strength development in a positive manner. An examination of the model also revealed the presence of interaction between voltage gradient and Na_2O content and the interaction between confining pressure and Na_2O content. However, the

quadratic effects of voltage gradient and confining pressure negatively affect compressive strength development. Fig. 5 and Fig. 6 represent the model set at different levels of total water content and confining pressure within the studied boundary.

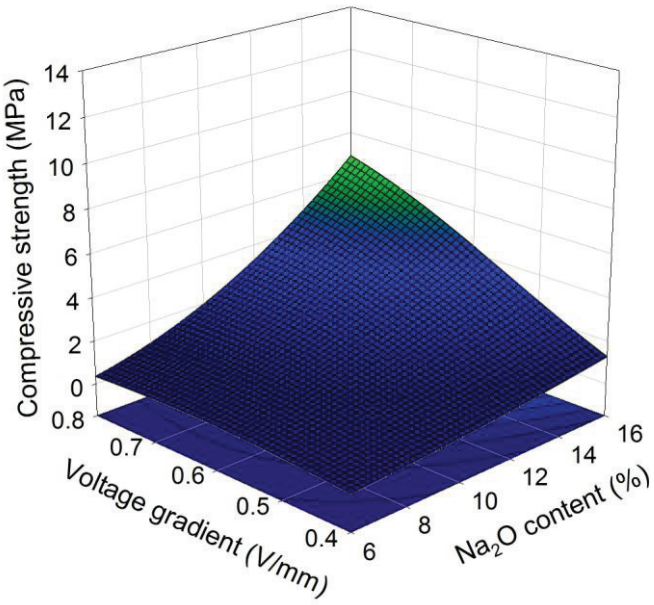

(Single column, 90 mm, fitting image and in colour)

Fig. 5. Response surface plot at constant 7% total water content and 5 MPa confining pressure

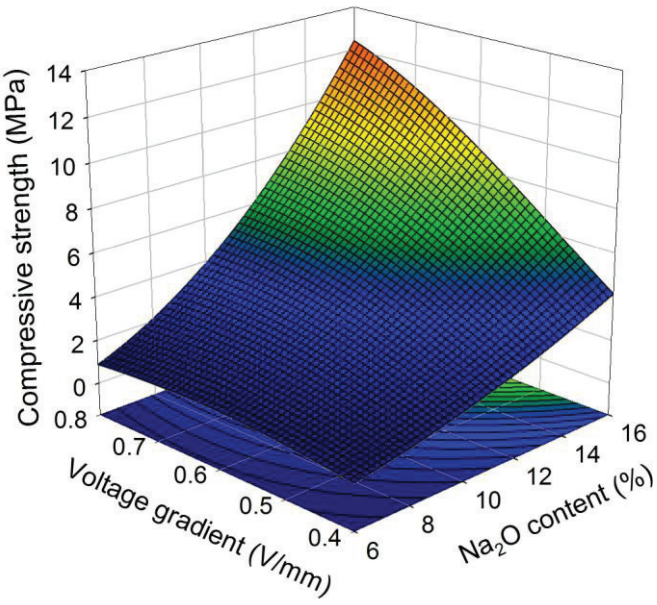

(Single column, 90 mm, fitting image and in colour)

Fig. 6. Response surface plot at constant 9% total water content and 10 MPa confining pressure

Na_2O content contributes the most to compressive strength development. It is expected for Na_2O content to provide the most strength contribution, since it is the only constituent directly involved in the alkali activation of fly ash [35]. The influential contribution of Na_2O content is in good agreement with De Vargas et al.'s (2011) [41] findings; the authors observed that alkali concentration was the most influential variable in the compressive strength development of alkali-activated materials.

Voltage gradient contributes the second most, almost half of the Na_2O content's contribution. Voltage gradient indirectly contributes to compressive strength development by increasing the reaction kinetics. This is in good agreement with Palomo et al. (2004) [32] findings, the authors observed that an increase in thermal energy corresponded with an increase in the rate of compressive strength gain.

It is interesting to note that, even though the Na_2O content and voltage gradient individually contribute significantly to compressive strength development in the studied system, their interaction provides additional significant contribution to compressive strength development. Therefore, Na_2O content and voltage gradient are two important independent variables during the manufacture of the NaOH-activated fly ash based mixture in the studied system.

Total water content, confining pressure and the interaction between confining pressure and Na_2O content contribute approximately the same amount; their contribution is rather small compared to Na_2O content and voltage gradient. Ahmari and Zhang (2012) [13] observed that an increase in confining pressure resulted in an increase in compressive strength; the authors explain that an increase in confining pressure leads to a higher degree of compaction of the mixture, which contributes to an increase in compressive strength. Ahmari and Zhang (2012) [13] also observed that an increase in water content resulted in an increase in compressive strength; the authors explain that a mixture with a higher water content provides more space (medium) for the formation of the alkali aluminosilicate gel than a mixture with lower water

content. The empirical model is in good agreement with Ahmari and Zhang's (2012) [13] findings.

3.2. Temperature rise and current density flow

The 2^4 central composite design produced a wide range of heating curves. The measured peak temperatures varied between 29.6 °C and 64.2 °C, and the time taken to reach the peaks varied between 7 and 140 minutes. Fig. 7 and Fig. 8 represent the heating curves of factorial design points set at 0.4 and 0.8 V/mm respectively.

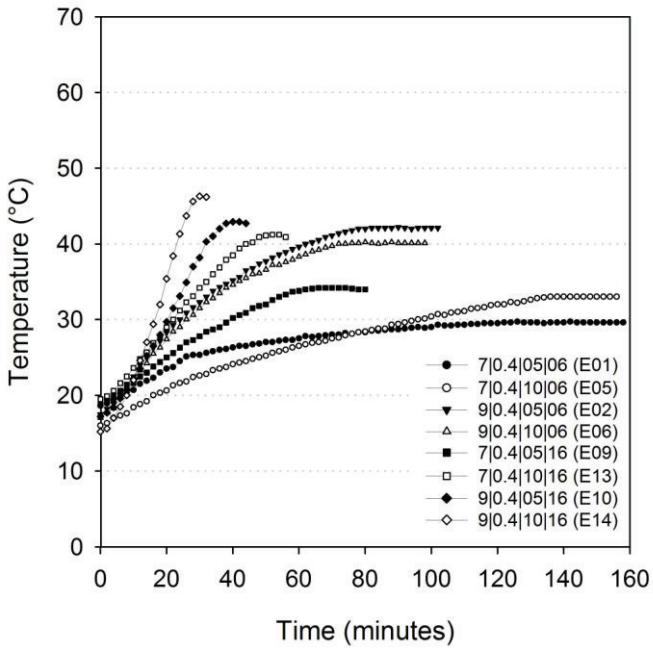

(Single column, 90 mm, fitting image)

Fig. 7. Temperature rise of 0.4 V/mm factorial design points

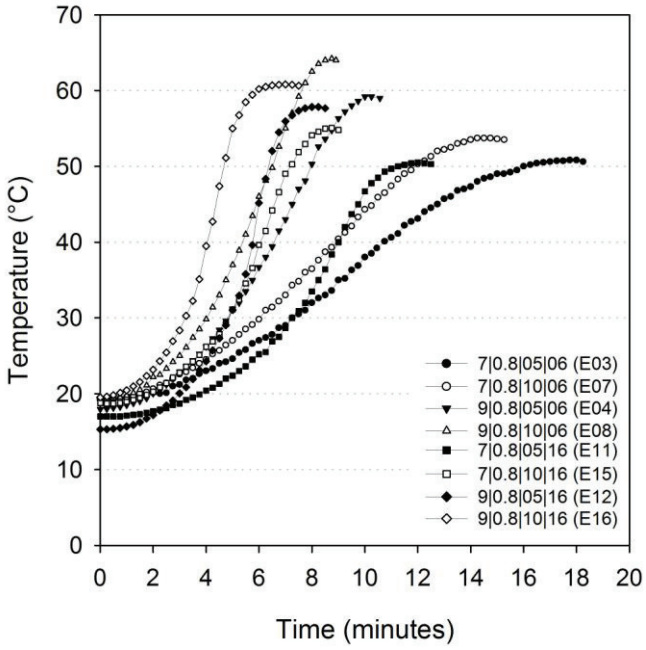

(Single column, 90 mm, fitting image)

Fig. 8. Temperature rise of 0.8 V/mm factorial design points

The different heating curves, obtained from the different combinations of low and high levels of the variables employed, indicate that none of the factors are unimportant. The design point set at all low levels, 7|0.4|05|06 (E01) (Fig. 4), resulted in the lowest peak temperature of 29.6 °C and, at 140 minutes, took the longest time to reach the peak (Fig. 7). This design point resulted in one of the lowest compressive strengths. In contrast, the design point set at all high levels, 9|0.8|10|16 (E16) (Fig. 4), resulted in the second highest peak temperature of 60.8 °C and, at 7 minutes, took the shortest period to reach the peak (Fig. 8). This design point resulted in the highest compressive strength.

The largest change in peak temperature is attributed to the change in voltage gradient and, to a lesser extent, to total-water-content. Confining pressure and Na_2O content contributed little to the change in peak temperatures. However, the influence of Na_2O content is evident in the rate of change in temperature. Samples with a higher Na_2O content (16%) reached their respective peak temperatures in a shorter duration than samples with a lower Na_2O content (6%). The lowest heating rate is attributed to the design point set at all four low levels,

7|0.4|05|06 (E01) (Fig. 4); a rate of 0.2 °C/minute (12.6 °C/hour) was observed. This is below the recommended maximum heating rate of 20 °C/hour, and is in the safe region of curing [14]. The highest heating rate observed was with the factorial design point set at all high levels, 9|0.8|10|16 (E16) (Fig. 4). A remarkable rate of 8.7 °C/minute (521.2 °C/hour) was observed, well above the recommended maximum heating rate. Although this rate is remarkable, it was short lived. A curing duration of only 7 minutes was possible before the temperature started dropping.

The factorial design points with 0.8 V/mm voltage gradients, steam was observed leaving the drainage paths of the confined-DEC set-up before the temperature started dropping. The generation of steam indicates movement of water within the mixture during curing, and this contributed to diminishing the conductive medium. Without a conductive medium, Joule heating cannot proceed and therefore the drop in temperature is a result of the diminishing conductive medium. This indicates the limited capability of the confined-DEC set-up under free drainage conditions to hold the expansive conductive medium under extreme heating rates.

Like the heating curves, the corresponding current density curves varied between the factorial design points. The extent of the influence of the variables mentioned follows a similar trend in the current density curves. This is expected, since electric conductivity is dependent on temperature. Fig. 8 and Fig. 9 represent the current density curves of factorial design points set at 0.4 and 0.8 V/mm respectively.

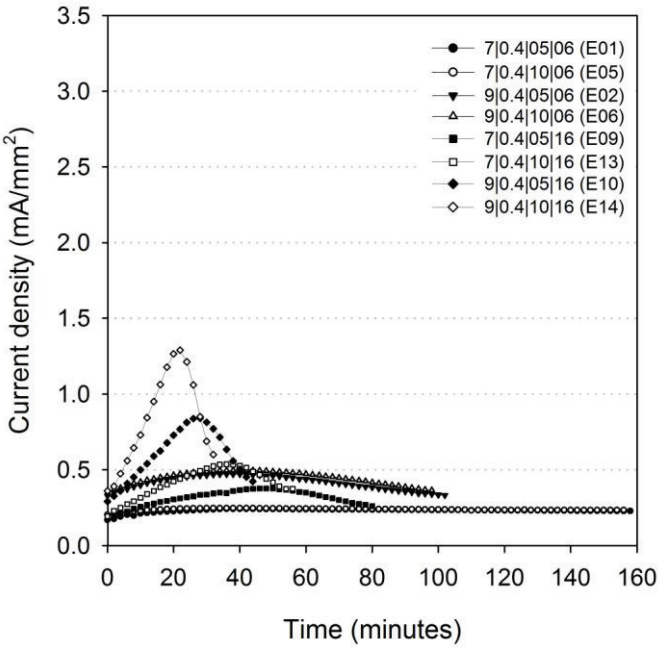

(Single column, 90 mm, fitting image)

Fig. 9. Current density flow of 0.4 V/mm factorial design points

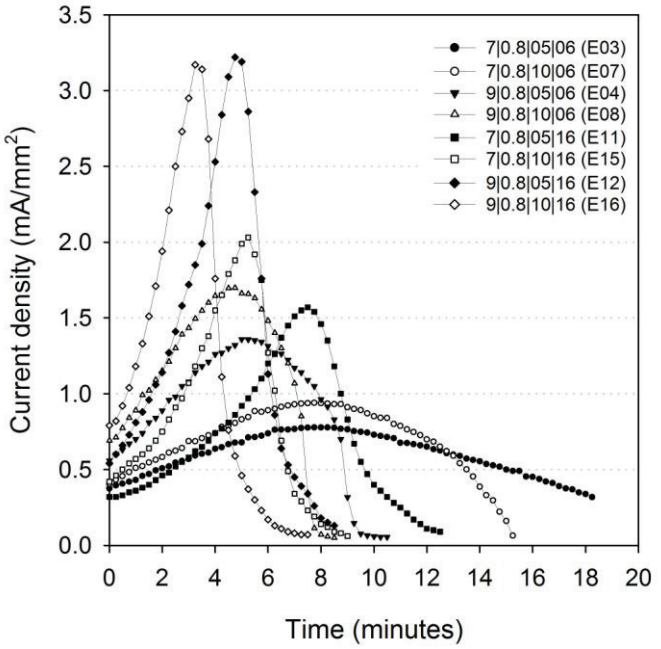

(Single column, 90 mm, fitting image)

Fig. 10. Current density flow of 0.8 V/mm factorial design points

The design point set at all low levels, 7|0.4|05|06 (E01) (Fig. 4), resulted in the lowest peak current density flow of 0.24 mA/mm^2 (Fig. 9) and also in the lowest temperature rise. In

contrast, the design point set at all high levels, 9|0.8|10|16 (E16) (Fig. 4), resulted in the second highest peak current density flow of 3.17 mA/mm^2 (Fig. 10) and in the second highest temperature rise. The largest change in peak current density flow is attributed to voltage gradient, followed by Na_2O content and total water content.

In all the design points, the current density flow initially increased, which is attributed to the increase in temperature of the conductive medium. The ion movement in a conductive medium increases with an increase in temperature, and, consequently, conductivity increases [15]. Design points with higher heating rates resulted in a sharper decline in current density flow once their respective peak current density was reached. With these design points, steam was observed shortly afterwards leaving the drainage paths of the confined-DEC set-up. Current density flow gives a more accurate time-related account of the change in the conductive medium because the parameter is measured throughout the mixture and not on the surface. There is a considerable time difference between the peak current density and peak temperature. This indicates that there is a delay in temperature reading of the actual temperature within the mixture. It also indicates that, since temperature rise is related to current flow, the true heating rate is significantly higher than the measured rate.

3.3. Other observation

Two distinct regions were observed immediately after the samples were crushed. These two distinct regions were also more prevalent in design points with higher heating rates and where steam leaving from the drainage path was noticed. There is a clear distinction between the inner-core (lighter shade of grey) and the outer-core (darker shade of grey). Fig. 11 depicts these two regions.

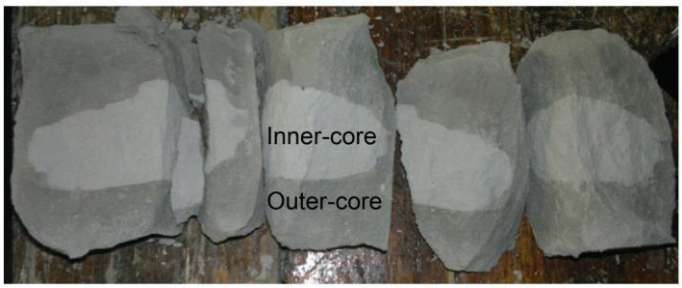

(Single column, 90 mm, fitting image and in colour)

Fig. 11. A crushed 50 mm cube immediately after the application of confined-DEC.

Darcy's empirical law of water movement in a homogenous material [42] can be used to describe the mechanism behind the two distinct regions. When there is no hydraulic gradient in a material over a distance, no water movement will occur. However, a movement of water will occur from a high-hydraulic pressure zone to a low-hydraulic pressure zone. Steam was noticed leaving the confined-DEC set-up from the drainage paths; in this case the drainage paths are thus the low-hydraulic pressure zone and the high-hydraulic pressure zone is generated within the mixture.

When a critical temperature is reached during curing, a hydraulic gradient sufficient for propelling the movement of the conductive medium from within the central region of the mixture to the drainage paths is raised. The raise of the critical hydraulic gradient occurs before a certain temperature rise has spread throughout the entire mixture and hence the two distinct regions are formed. The diminishment of the conductive medium prevents further temperature rise (Joule heating) in the outer-core region, creating the two distinct regions. The critical temperature that initiates the movement of the conductive medium does not necessarily happen around 100 °C, which is the boiling point of water. Atiş et al. (2015) [43] observed that the compressive strength development of mixtures with sufficient NaOH concentrations were not severely affected at elevated temperature curing regimes of 105 °C and higher. They explain that an increase in NaOH concentration increases the boiling point of the NaOH activator solution.

During the application of DEC, heat rises volumetrically throughout the mixture, but the heat in the centre of the mixture rises at a higher rate since it is the most insulated. Kafry (1993) [15] explains that DEC induces an inverted temperature gradient unlike conventional accelerated curing techniques, and Heritage (2001) [20] observed that with DEC, the maximum temperature during curing is always in the central region of the mixture. With microwave curing, Somaratna et al. (2010) [16] also observed an inverse temperature gradient; the highest temperature was observed to be in the centre of the mixture. They explain that the inverted temperature gradient is due to the temperature differential between the mixture and the microwave cavity; this introduces convective and radiative heat loss between the exposed surface of the mixture and the microwave cavity. In the confined-DEC set-up, however, the electrodes and the non-conductive material which confine the mixture do not correspondingly increase in temperature during curing and hence a temperature differential between the mixture and the confining material is created. The non-conductive material provides better insulating properties than the electrodes. The electrodes act as heat sinks, contributing to a greater heat loss than the non-conductive material. From Fig. 10 it is evident that more heat loss occurred in the two regions facing the electrodes. The inner-core grew broader towards the face of the non-conductive material than towards the face of the electrodes, the two regions that were more susceptible to heat loss.

3.4. Beyond the studied boundaries

The empirical model revealed that increasing the magnitude of each independent variable from a low level to a high level resulted in an increase in compressive strength development. The design point set at all low levels, 7|0.4|05|06 (E01) (Fig. 4), resulted in the lowest compressive strength and the design point set at all high levels, 9|0.8|10|16 (E16) (Fig. 4), resulted in the highest compressive strength. However, an investigation beyond the studied

boundaries of the empirical model revealed the limitations of confined-DEC under free drainage conditions.

When the magnitude of each independent variable was further increased beyond the studied boundaries, compressive strength development did not increase. A new design point was investigated with the following increased parameters: 11% total water content, 1.2 V/mm voltage gradient, 15 MPa confining pressure and 20% Na_2O content; the resultant average compressive strength was 9.8 MPa, slightly lower than that of 9|0.8|10|16 (E16) (Fig. 4), which was 11.5 MPa.

Fig. 12 and Fig. 13 depict the temperature profile and current density flow respectively of the design point 9|0.8|10|16 (E16) (Fig. 4) and the new design point with increased parameters, 11|1.2|15|20. Even though the new design point, 11|1.2|15|20, produced a higher temperature rise and also contained more Na_2O content than 9|0.8|10|16 (E16) (Fig. 4), the final strength of 11|1.2|15|20 was lower than that of 9|0.8|10|16 (E16).

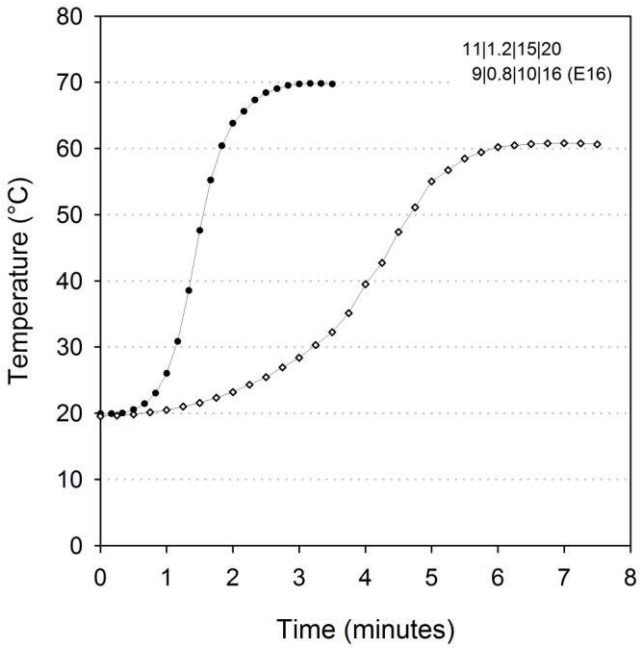

(Single column, 90 mm, fitting image)

Fig. 12. Temperature profile comparison.

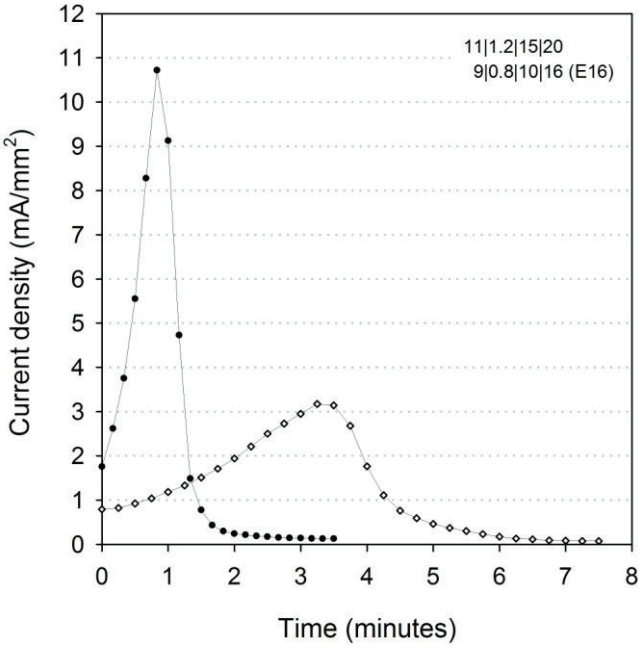

(Single column, 90 mm, fitting image)

Fig. 13. Current density flow profile comparison

A more violent steam burst was observed for 11|1.2|15|20 than for 9|0.8|10|16 (E16) (Fig. 4). The rapid change in the current density flow of 11|1.2|15|20 indicates that the conductive medium rapidly diminished. The violent movement of water probably prevented to a certain extent the formation of the alkali aluminosilicate gel, even though a considerable temperature rise was induced. After all, the formation of alkali aluminosilicate gel takes place in a static medium. This contributed to a decrease in compressive strength development. The inability of the confined-DEC set-up under free drainage conditions to hold a conductive medium at extreme heating rates demonstrates the curing technique's limitations.

The investigation revealed the limitations of confined-DEC under free drainage conditions. However, the investigation consisted of only 50 mm cubes, and, for much thicker mixtures with the same induced conditions, the result could be higher compressive strength development. Increasing the volume of the mixture to for instance 100 x 100 x 100 mm, will increase not only the capillarity migration path of the conductive medium to the drainage

path, but also the amount of force required to push out the increased volume of the conductive medium. Higher maximum temperatures will therefore be associated with thicker mixtures.

3.5. Compressive strength development and water absorption

Fig. 14 depicts the compressive strength development and water absorption of factorial design point 9|0.8|10|16 (E16).

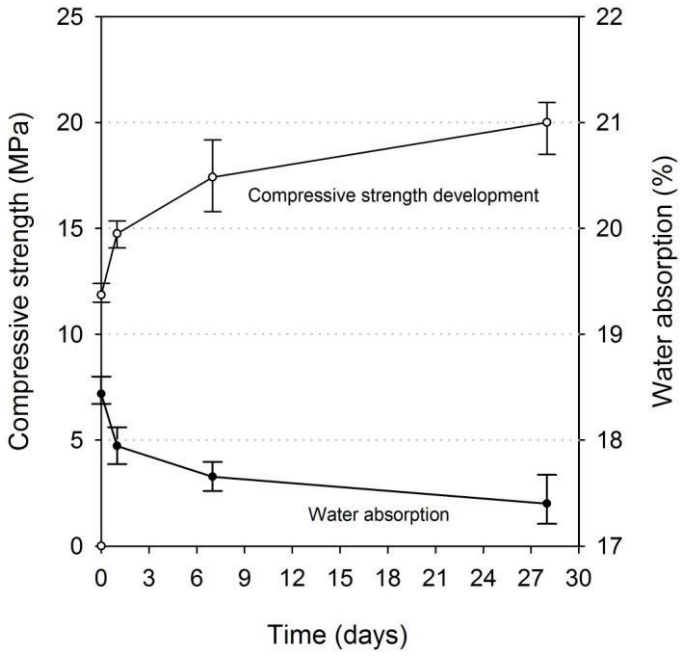

(Single column, 90 mm, fitting image)

Fig. 14. Compressive strength development and water absorption of factorial design point 9|0.8|10|16 (E16)

After approximately 7 minutes under confined-DEC, the samples acquired an average compressive strength of 11.5 MPa. The samples continued to increase in compressive strength development but at a lower rate, reaching an average compressive strength of 20.1 MPa at 28 days. This increase in compressive strength indicates that the formation of the alkali aluminosilicate gel was still taking place after the application of confined-DEC had ended; the alkali aluminosilicate gel is the main product of reaction giving the mechanical

properties [44]. The formation of the alkali aluminosilicate gel depends on temperature as well as age [41]. Somna et al. (2011) [45] observed that compressive strength increased with an increase in age of NaOH-activated fly ash samples cured at room temperature. The observance of steam leaving from the drainage paths of the confined-DEC set-up indicates a reduction in water within the mixture. However, some water was still present in the mixture after curing because without water availability, the formation of the alkali aluminosilicate gel cannot proceed [39]. The compressive strength development correlates with the change in water absorption of the samples. As the amount of alkali aluminosilicate gel increases, the material becomes more compact, reducing its porosity. Ahmari and Zhang (2012) [13] explain that a larger amount of alkali aluminosilicate gel leads to lower porosity and permeability.

4. Conclusion

The application of the confined-DEC technique in the rapid accelerated curing of NaOH-activated fly ash based brick mixtures is a unique concept that has great potential for high-volume fly ash utilisation. A 2^4 central composite design was employed to recognise the influence of each variable and variable interaction on the rapid compressive strength development of NaOH-activated fly ash based brick mixtures subjected to confined-DEC. Based on the study, the different combinations of total water content, voltage gradient, confining pressure and Na_2O content generated a unique response for each design point. The empirical model revealed the importance of Na_2O content, voltage gradient and their interaction in contributing to compressive strength development. Confining pressure and total water content played a smaller role in compressive strength development in the studied system.

The rapid strength gain is apparent from the increased reaction kinetics, which are as a result of the rapid rise in temperature within the mixture. The variable voltage gradient has the greatest influence on temperature rise, and the influence of the Na_2O content is evident in the heating rate, as an increase in the Na_2O content resulted in an increase in the heating rate. The same variable voltage gradient responsible for the greatest influence on temperature is also responsible for the greatest influence on the current density flow. This is expected since conductivity is dependent on temperature. Variable Na_2O content and total water content also show notable influence on the current density flow, but to a lesser extent.

The best factorial design point, 9|0.8|10|16 (E16) (Fig. 4), obtained a compressive strength of 11.5 MPa in 7 minutes after the application of confined-DEC. The considerable decrease in curing duration is desirable in the masonry industry. The same design point continued to increase in compressive strength development to 20.1 MPa at 28 days.

The confined-DEC technique is certainly a promising approach in the rapid accelerated curing of NaOH-activated fly ash based brick mixtures. However, under free drainage conditions, confined-DEC's potential is limited, due to its inability to hold the expansive conductive medium, which consequently leads to a loss in compressive strength under extreme heating rates.

The dangerous combination of a strong alkaline solution, steam bursts and live electricity could also impede the development of this concept as an alternative manufacturing approach. However, its implementation can take place in a safe, controlled environment, specifically in design industrial plants, which is usually the case for mass production of masonry units. Confined-DEC also conveniently goes hand-in-hand with press moulding, the production method for high-volume fly ash brick mixtures. This technique also should not be limited to the manufacture of masonry units and can be extended to the manufacture of rail sleepers and other precast civil engineering elements. Undesirable long shifts associated with oven curing reduced to a matter of minutes with the combination of confined-DEC and the binding

mechanism of NaOH activation of fly ash provides an attractive alternative for high-volume fly ash utilisation through rapid accelerated curing.

This is a unique concept with great room for future research. The second part of this study (Part 2: Confined-DEC versus oven curing [46]) will be published as a follow-up to Part 1. Part 2 focuses on the assessment of the structural differences between samples prepared with conventional oven curing and samples prepared with confined-DEC.

5. Acknowledgements

The authors would like to thank Bogdan Ziolkowski and Werner Breytenbach for the fabrication of the confined-DEC set-up.

6. References

[1] Eskom Integrated Report 2014. http://integratedreport.eskom.co.za/pdf/full-integrated.pdf (accessed 07.12.2015).

[2] J.G.S. van Jaarsveld, J.S.J. van Deventer, L. Lorenzeni, The potential use of geopolymeric materials to immobilise toxic metals: part I. Theory and applications, Miner. Eng. 10 (7) (1997) 659–669.
http://dx.doi.org/10.1016/S0892-6875(97)00046-0

[3] T. Hemalatha, A. Ramaswamy, A review on fly ash characteristics – Towards promoting high volume utilization in developing sustainable concrete, J. Clean. Prod. 147 (2017) 546–559.
http://dx.doi.org/10.1016/j.jclepro.2017.01.114

[4] S. Naganathan, A. Yousef, O. Mohamed, K.N. Mustapha, Performance of bricks made using fly ash and bottom ash, Constr. Build. Mater. 96 (2015) 576–580.

http://dx.doi.org/10.1016/j.conbuildmat.2015.08.068

[5] L. Zhang, Production of brick from waste materials – A review, Constr. Build. Mater. 47 (2013) 643–655.

http://doi.org/10.1016/j.conbuildmat.2013.05.043

[6] C. Ferone, F. Colangelo, R. Cioffi, F. Montagnaro, L. Santoro, Mechanical performances of weathered coal fly ash based geopolymer bricks, Procedia Eng. 21 (2011) 745–752.

http://dx.doi.org/10.1016/j.proeng.2011.11.2073

[7] M.B. Diop, M.W. Grutzeck, Low temperature process to create brick, Constr. Build. Mater. 22 (6) (2008) 1114–1121.

http://dx.doi.org/10.1016/j.conbuildmat.2007.03.004

[8] H. Liu, W. Burkett, K. Haynes, Improving Freezing and Thawing Properties of Fly Ash Bricks, World of Coal Ash (WOCA) Conference, Lexington, Kentucky, 2005.

[9] A.E. Campbell, Chemical, physical and mineralogical properties associated with the hardening of some South African fly ashes, MSc dissertation, Department of Geological Sciences, University of Cape Town, Cape Town, South Africa, 1999.

[10] S. Shi, Y. Bai, H. Li, D.L. Xu, P.A.M. Basheer, Comparative Study of Alkali-Activated Fly Ash Manufactured Under Pulsed Microwave Curing and Thermal Oven Curing, 4th International Conference on the Durability of Concrete Structures, 2014.

[11] J. Shekhovtsova, E.P. Kearsley, M. Kovtun, Effect of activator dosage, water-to-binder-solids ratio, temperature and duration of elevated temperature curing on the compressive strength of alkali-activated fly ash cement pastes, J. S. Afri. Inst. Civ. Eng. 56 (3) (2014) 44–52.

[12] P. Chindaprasirt, U. Rattanasak, S. Taebuanhuad, Role of microwave radiation in curing the fly ash geopolymer, Adv. Powder Technol. 24 (3) (2013) 703–707.

http://dx.doi.org/10.1016/j.apt.2012.12.005

[13] S. Ahmari, L. Zhang, Production of eco-friendly bricks from copper mine tailings

through geopolymerization, Constr. Build. Mater. 29 (2013) 323–331. http://dx.doi.org/10.1016/j.conbuildmat.2011.10.048

[14] ACI, Committee 517, Accelerated Curing of Concrete at Atmospheric Pressure-State of the Art, Am. Concr. Inst. (1992) ACI 517.2R.

[15] I.D. Kafry, Direct Electric Curing of Concrete: Basic Design, Whittles Publishing, Latheronwheel, 1993.

[16] J. Somaratna, D. Ravikumar, N. Neithalath, Response of alkali activated fly ash mortars to microwave curing, Cem. Concr. Res. 40 (12) (2010) 1688–1696. http://doi.org/10.1016/j.cemconres.2010.08.010

[17] J. Davidovits, J.J. Legrand, Process for agglomerating compressible mineral substances under the form of powder, particles or fibres, US Patent 4028454, 1977.

[18] K.R. Backe, O.B. Lile, S.K. Lyomov, Characterizing curing cement sluries by electrical conductivity, SPE Drill. Complet. 16 (04) (2001) 201-207. http://doi.org/10.2118/74694-PA

[19] J.G. Wilson, N.K. Gupta, Equipment for the investigation of the accelerated curing of concrete using direct electrical conduction, Meas. 35 (2004) 243-250. http://doi.org/10.1016/j.measurement.2003.11.002

[20] I. Heritage, Direct electric curing of mortar and concrete, PhD dissertation, School of the Built Enviroment, Napier University, Endinburg, UK, 2001.

[21] S. Bredenkamp, D. Kruger, G.L. Bredenkamp, Direct electric curing of concrete, Mag. Concr. Res. 45 (165) (1993) 71–74. http://dx.doi.org/10.1680/macr.1993.45.162.71

[22] S.S. Wadhwa, L.K. Srivastava, D.K. Gautam, D. Chandra, Direct electric curing of in situ concrete, Batim. Int. Buil. Res. Pract. 15 (1–6) (1987) 97–101. http://dx.doi.org/10.1080/09613218708726799

[23] P.V. Sivapullaiah, H. Lakshmikantha, Properties of Fly Ash as Hydraulic Barrier, Soil Sediment Contam. 13 (5) (2004) 391–406.
doi: 10.1080/10588330490500437.

[24] P.J.J. Domone, P.L.J. Illston, Construction materials: their nature and behaviour, fourth ed., Spon press, Abingdon, Oxon, 2010.

[25] R.T. Belden, M. Cristallo, G. Ittmann, R. Ittmann, Bricks and method of forming bricks with high coal ash content using a press mold machine and variable firing trays, US Patent 2012/0031306 A1, 2012.

[26] C. Shi, D. Roy, P. Krivenko, Alkali-Activated Cements and Concretes, Taylor & Francis, Oxon, Abingdon, 2006.

[27] T. Phoo-Ngernkham, A. Maegawa, N. Mishima, S. Hatanaka, P. Chindaprasirt, Effects of sodium hydroxide and sodium silicate solutions on compressive and shear bond strengths of FA-GBFS geopolymer, Constr. Build. Mater. 91 (2015) 1–8.
http://dx.doi.org/10.1016/j.conbuildmat.2015.05.001

[28] T. Bakharev, Geopolymeric materials prepared using Class F fly ash and elevated temperature curing, Cem. Concr. Res. 35 (6) (2005) 1224–1232.
http://dx.doi.org/10.1016/j.cemconres.2004.06.031

[29] M. Kovtun, M. Ziolkowski, J. Shekhovtsova, E. Kearsley, Direct electric curing of alkali-activated fly ash concretes: a tool for wider utilization of fly ashes, J. Clean. Prod. 133 (2016) 220–227.
http://dx.doi.org/10.1016/j.jclepro.2016.05.098

[30] G. Whissell, Compaction device for concrete block molding machine, (1989) US Patent 4802836.

[31] D.C. Montgomery, Design and Analysis of Experiments, eighth ed., John Wiley & Sons, 2012.

[32] A. Palomo, S. Alonso, A. Fernandez-Jiménez, I. Sabrados, J. Sanz, Alkaline Activation

of Fly Ashes: NMR Study of the Reaction Products, J. Am. Ceram. Soc. 87 (6) (2004) 1141–1145.

http://dx.doi.org/10.1111/j.1551-2916.2004.01141.x

[33] SANS 1215:2008, Concrete masonry units, 1.4 ed., Standards South Africa, Pretoria, South Africa, 2008.

[34] Z. Zuhua, Y. Xiao, Z. Huajun, C. Yue, Role of water in the synthesis of calcined kaolin-based geopolymer, App. Clay Sci. 43 (2) (2009) 218–223.

http://dx.doi.org/10.1016/j.clay.2008.09.003

[35] A. Fernández-Jiménez, A. Palomo, Composition and microstructure of alkali activated fly ash binder: Effect of the activator, Cem. Concr. Res. 35 (10) (2005) 1984–1992.

http://dx.doi.org/10.1016/j.cemconres.2005.03.003

[36] M.C. Knirsch, C.A. dos Santos, A.A.M. de Oliveira Soares Vicente, T.C.V. Penna, Ohmic heating - a review, Trends Food Sci. Technolog. 21 (9) (2010) 436–441.

http://dx.doi.org/10.1016/j.tifs.2010.06.003

[37] D. Ravikumar, S. Peethamparan, N. Neithalath, Structure and strength of NaOH activated concretes containing fly ash or GGBFS as the sole binder, Cem. Concr. Compos. 32 (6) (2010) 399–410.

http://dx.doi.org/10.1016/j.cemconcomp.2010.03.007

[38] U. Rattanasak, P. Chindaprasirt, Influence of NaOH solution on the synthesis of fly ash geopolymer, Miner. Eng. 22 (12) (2009) 1073–1078.

http://dx.doi.org/10.1016/j.mineng.2009.03.022

[39] G. Kovalchuk, A. Fernández-Jiménez, A. Palomo, Alkali-activated fly ash: Effect of thermal curing conditions on mechanical and microstructural development - Part II, Fuel 86 (3) (2007) 315-322.

http://dx.doi.org/10.1016/j.fuel.2006.07.010

[40] Stat-Ease Inc., Design-Expert Software Version 10.0, Minneapolis, MN, 2016.

[41] A.S. De Vargas, D.C.C. Dal Molin, A.C.F. Vilela, F.J. da Silva, B. Pavão, H. Veit, The effects of Na_2O/SiO_2 molar ratio, curing temperature and age on compressive strength, morphology and microstructure of alkali-activated fly ash-based geopolymers, Cem. Con. Comp. 33 (6) (2011) 653–660.
http://dx.doi.org/10.1016/j.cemconcomp.2011.03.006

[42] J.A. Knappett, R.F. Craig, Craig's soil mechanics, Spon Press, Abingdon, Oxon, 2012.

[43] C.D. Atiş, E.B. Görür, O. Karahan, C. Bilim, S. İlkentapar, E. Luga, Very high strength (120 MPa) class F fly ash geopolymer mortar activated at different NaOH amount, heat curing temperature and heat curing duration, Constr. Build. Mater. 96 (2015) 673–678.
http://dx.doi.org/10.1016/j.conbuildmat.2015.08.089

[44] M. Criado, A. Fernandez-Jimenez, A.G. de la Torre, M.A.G. Aranda, A. Palomo, An XRD study of the effect of the SiO_2/Na_2O ratio on the alkali activation of fly ash, Cem. Concr. Res. 37 (5) (2007) 671–679.
http://dx.doi.org/10.1016/j.cemconres.2007.01.013

[45] K. Somna, C. Jaturapitakkul, P. Kajitvichyanukul, P. Chindaprasirt, NaOH-activated ground fly ash geopolymer cured at ambient temperature, Fuel 90 (6) (2011) 2118–2124.
http://dx.doi.org/10.1016/j.fuel.2011.01.018

[46] M. Ziolkowski, M. Kovtun, Confined-Direct Electric Curing of NaOH-activated fly ash brick mixtures under free drainage conditions. Part 2: Confined-DEC versus oven curing, Submitted to Construction and Building Materials, 2017.